Journal of Applied Polymer Science

Preparation and Enhanced Electrochemical Properties of Ag/Polypyrrole Composites Electrode Materials

Jun Liu,[1] Mei Li,[1,2,3] Yunqiang Zhang,[1] Lanlan Yang,[1] Jinshao Yao[1,2,3]

[1]School of Materials Science and Engineering, Shandong Polytechnic University, Jinan 250353, People's Republic of China
[2]Shandong Provincial Key Laboratory of Processing and Testing Technology of Glass and Functional Ceramics, Shandong Polytechnic University, Jinan 250353, People's Republic of China
[3]Key Laboratory of Amorphous and Polycrystalline Materials, Shandong Polytechnic University, Jinan 250353, People's Republic of China
Correspondence to: M. Li (E-mail: limei@spu.edu.cn)

ABSTRACT: Ag/polypyrrole (PPy) composites were synthesized with different dispersants via interface polymerization method. The morphology of the composites was investigated by scanning electron microscopy and transmission electron microscopy, and the results showed that the dispersant had strong effect on the morphology of the obtained composites. The structure of the products was characterized by Fourier transform infrared spectroscopy, and X-ray diffraction. The specific capacitance and impedence of Ag/PPy composites electrode was evaluated through charge/discharge measurements and electrochemical impedance spectroscopy, respectively. Electrochemical performances indicated that Ag/PPy composite electrode used polyvinyl alcohol as dispersant exhibited the highest specific capacitance of 635.5 F/g at a current density of 2.45 mA/g, which provided potential application as supercapacitor materials. © 2013 Wiley Periodicals, Inc. J. Appl. Polym. Sci. 000: 000–000, 2013

KEYWORDS: composites; conducting polymers; electrochemistry

Received 8 December 2012; accepted 29 January 2013; published online
DOI: 10.1002/app.39102

INTRODUCTION

In recent years, the electrically conducting composites have attracted intensive attentions of researchers because of their potential applications in various fields, such as sensors, actuators, and electric devices.[1–4] Among these electrically conducting polymers such as polypyrrole (PPy),[5,6] polyaniline ,[7–9] polythiophene,[10] poly(3,4-ethylenedioxythiophene)[11] and poly(*p*-phenylene vinylene),[12] PPy is known as one of the most important conducting polymers owing to its high conductivity, easy preparation, good environmental tolerance, and a large variety of applications.[13] Accordingly, the fabrication of metal and PPy nanomaterials has become an important branch of electrically conducting composite researches. It is well known that nanoparticles have attracted increasing interests because one-dimensional (1-D) nanomaterials can offer a range of unique advantages in electrochemical- and energy-related fields. Complex nanostructures have been increasingly reported in recent years because they could offer better electrochemical performance than single-structured materials. For example, Ag/PPy core–shell nanoparticles have been synthesized via *in situ* chemical oxidation of pyrrole based on mercaptocarboxylic acid-capped Ag nanoparticles colloid.[14] PPy-coated Au nanoparticles were synthesized by using Martin Möller group using $HAuCl_4$ as an oxidizing agent with the formation of very fine Au nanoparticles within the core.[15]

Herein, we report the synthesis of PPy-coated Ag nanocomposites by using the redox reaction of silver nitrate and pyrrole via interface polymerization in the presence of dispersant. In this report, two phases of CCl_4-containing pyrrole and water-dissolved $AgNO_3$ and dispersant acted as the reactive biphasic system to prepare PPy-coated Ag nanocomposites.

EXPERIMENTALS AND CHARACTERIZATION

Materials

Pyrrole, carbon tetrachloride (CCl_4), polyethylene glycol (PEG), polyvinylpyrrolidone (PVP), and polyvinyl alcohol (PVA) were purchased from Sinopharm Chemical Reagent. Silver nitrate (99.8%) was purchased from Beijing Chemical Plant. Pyrrole monomer was distilled under reduced pressure before using, and other reagents were used as received without further treatment.

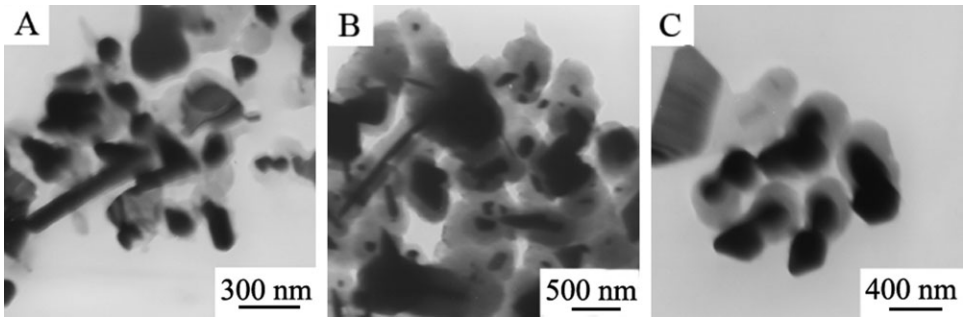

Figure 1. TEM images of samples.

Preparation of Ag/PPy Nanocomposites

In a typical procedure for the synthesis of PPy-coated Ag nanocomposites, 0.07 mL of pyrrole was dissolved in 10 mL of CCl_4, 0.12 g $AgNO_3$ and 0.2 g dispersant were dissolved in 10 mL of deionized water, the two solutions were mixed in the beaker, and an interface was generated immediately between two solutions. Brownish black PPy-coated Ag nanocomposites were formed at the interface and then some black particles gradually diffused into the upper aqueous phase. The reaction was allowed to proceed for 72 h at room temperature. The product was first ultrasonicated and then the aqueous phase was centrifugated at 10,000 rpm for 30 min. The bottom layer in the centrifuge tube was collected as coarse product. After washing with acetone and ethanol and repeating the ultrasonication and centrifugation, the final product was obtained. The product was dried at 60°C in vacuum for 12 h. Sample A is fabricated with PVP as dispersant and in a similar manner samples A, B, and C are prepared with PEG and PVA as dispersants, respectively. The concentration of all of the three dispersants is 2%.

Characterization

The morphology of the product was directly observed with scanning electron microscopy (SEM) (FEIco-Holland, JSM-6700F) and transmission electron microscopy (TEM) (JEOL, JEM-1011). An X-ray diffraction (XRD) pattern was taken with a Bruker D8 ADVANCE XRD instrument at a 10°/min scanning speed from 20 to 80°. Fourier transform infrared spectroscopy (FTIR) spectra of the samples were obtained with a Shimadzu FTIR-8400s spectrophotometer in the range of 4000–500 cm^{-1} and the sample was impressed into KBr pellets. The composites for fabricating positive electrode were prepared by mixing active materials (80 wt %), carbon blacks (10 wt %), and polyvinylidene fluoride (10 wt %) and stirring at 25°C for 1 h to mix thoroughly. The materials were then coated on the surface of nickel foam (1.5 cm^2), dried at 60°C for 8 h, and pressed at 15 MPa to get PPY composite electrode. The electrical performance of the synthesized samples was determined by the ZL10 LCR instrument (Shanghai Instrument Research Institute, China).

RESULTS AND DISCUSSION

Morphology and Structure of Ag/PPy Composites

Figure 1 shows the TEM images of the three samples. In Figure 1, the clear dark–light contrast can be seen, which belongs to PPy shells (light contrast) and silver cores (dark contrast), respectively. PPy-coated Ag nanocomposites were synthesized through the redox reaction of $AgNO_3$ and pyrrole monomer. Many differences including size and morphology of the Ag/PPy composites could be observed in Figure 1, illustrating that the dispersant has a strong effect of the resultant products because the whole polymerization process of the three samples is the same except dispersants. As shown in Figure 1(A), when the PVP was used as a dispersant, the obtained Ag/PPy nanocomposites were composed of the rod with diameter of 100 nm and triangular particles of 100–200 nm. The rod is actually a smooth core about 100 nm in diameter and a surrounding sheath about 50 nm in thickness, and the contrast between surrounding polymer and inner core can be easily observed. Figure 1(B) shows the size of the resultant particles was about 100–300 nm and the diameter of the generated rod was about 100 nm with the length of tens of micrometers. As shown in Figure 1(C), a typical core–shell structure was formed because of the addition of PVA. The product displays a darker core sheathed with lighter layer which suggests the formation of core–shell composites. The outer thickness is ~100 nm and the diameter of the central core of the composites is about 200 nm.

The morphology of the samples was further examined by SEM images as shown in Figure 2. Some polymers exhibit a rod-like morphology with diameter ranging from 100 to 200 nm consisting of particle blocks and more polymer particles congregate into bumps owing to different dispersants as shown in Figure 2(A,B). In Figure 2(B), the linear product is clear and the coaxial nanowires come into existence of which length and diameter are about 10 μm and 200 nm, respectively. Figure 2(C) shows that Ag/PPy composites are microspheres with diameter about 200–300 nm and uniform core–shell structure formed within the microspheres.

The XRD pattern of the nanocomposites indicated the crystal structure of the resulting polymer and the incorporation of the silver nanoparticles (Figure 3). Figure 3(D) shows the XRD patterns of silver, and in the other three curves, the diffraction peak at 2θ value of 24° was characteristic peak of the doped amorphous PPy,[16–18] and at the diffraction lines of 2θ = 38.5, 44.5, 64.7, and 77.7° were attributed to the (111), (200), (220), and (311) planes of the standard cubic phases of silver, respectively.[19,20] Owing to the higher scattering intensity of the metal nanoparticles compared to the amorphous organic PPy structures, the peaks assigned to the silver crystal plains appear with a higher intensity than the bands of PPy.

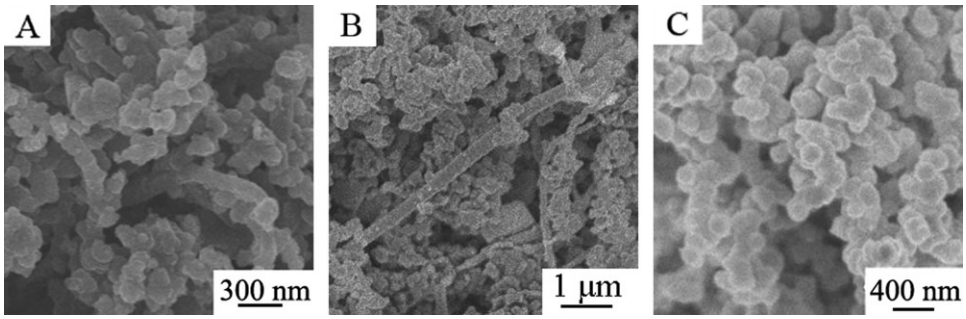

Figure 2. SEM images of samples.

The characteristic absorptions of PPy in the Ag/PPy composites nanoparticles are shown in Figure 4 in which the peaks located at 1543 and 1396 cm^{-1} are attributed to the pyrrole ring stretching and the conjugated C—N stretching mode, respectively.[21] The peak at 1170 cm^{-1} was related to C—N stretching wagging vibrations.[22] The peak at 910 cm^{-1} was owing to the ring deformation. The peaks at 1294 and 1043 cm^{-1} are related to the in-plane vibrations of =C—H and the peak at 788 cm^{-1} is attributed to C—H wagging vibration.[23] These results indicated the PPy was polymerized during the process at room temperature.

According to the literature, the dispersant has a strong effect on the size and morphology of the resultant products, without which the core shell–structure could not be formed.[24,25] It is well known that specific functional groups can be used to induce coating during the precipitation and surface reactions on the cores. There are three requirements for preparing Ag/PPy composites through the above one-step polymerization process as shown in Figure 5. First, polymerization of pyrrole into PPy and the reduction $AgNO_3$ to silver should occur simultaneously. Second, core–shell structures can be formed in this system. Third, pyrrole monomer can stably polymerize *in situ* on the surface of silver nanowires or silver particles. As shown in Figure 5, the silver ions interact with negative group of the dispersants first arose from electrostatic attraction, then reduced to silver atoms with dispersant adsorbed on the surface, and at the same time pyrrole radical cation was formed. During the synthetic process, the adsorbed dispersant might provide active sites on the silver particles and pyrrole radical cation so as to influence the morphology of the Ag/PPy composites.[26]

Electrochemical Performances of Ag/PPy Composites

The specific capacitance of the composites electrode was calculated from the discharge cycle of the typical voltage–time response curve in cyclic charge–discharge measurements using the following equation:

$$Cm = (i \times \Delta t)/(\Delta V \times m) \quad (1)$$

where C_m is the specific capacitance obtained from discharge cycle of constant current charge/discharge measurements, i is the constant current, Δt is the discharge time, ΔV is the potential range, and m is the mass of the sample.[27,28]

Figure 6(A–C) shows the galvanostatic charge–discharge curves of three composite electrodes at the current density of 2.45 mA g^{-1}. The discharge time increases in the order of A < B < C, and it can be calculated based on Figure 6 in which the specific capacitances of these electrodes are 15.6, 347.6, and 635.5 F/g,

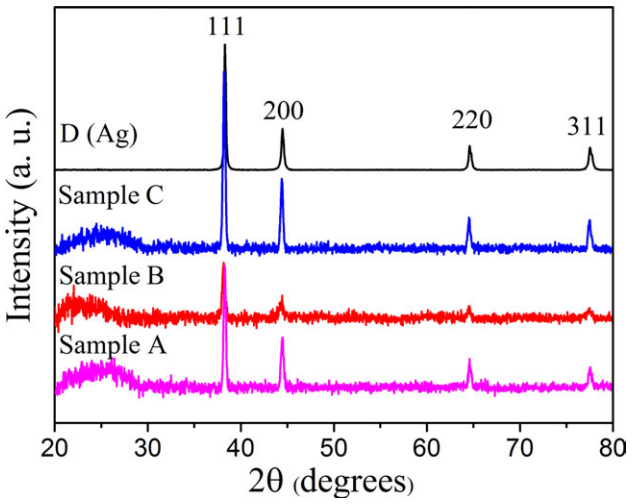

Figure 3. XRD patterns of Ag and samples. [Color figure can be viewed in the online issue, which is available at wileyonlinelibrary.com.]

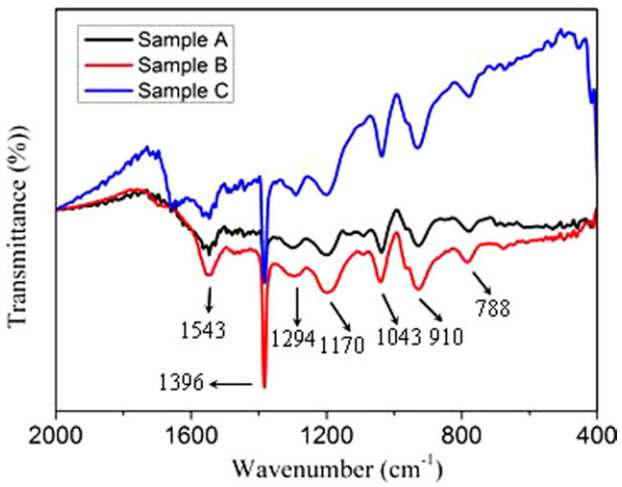

Figure 4. FTIR spectra of samples. [Color figure can be viewed in the online issue, which is available at wileyonlinelibrary.com.]

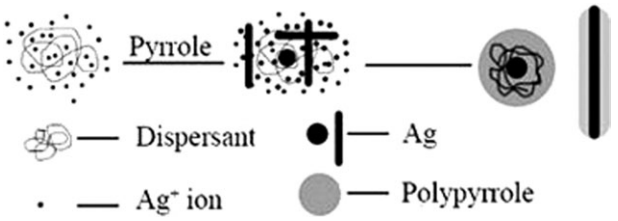

Figure 5. Schematic illustration of the formation process of Ag/PPy composites.

respectively. The high-specific capacitance value of samples B and C indicates that the different structures would be responsible for the permeation of electrolyte within the electrode. Hence, this composite electrode was more favorable for the applications of supercapacitors in low current density. It is significant for the electrode material that it can afford the higher specific capacitance, and hence Ag/PPy composite electrode could be a potential anode material for lithium battery.[29,30]

The specific capacitance of the composite electrode decreased with cycle number as shown in Figure 7. The specific capacitance retentions of samples A, B, and C after 50 cycles were 93, 95, and 97% of the initial value, respectively. The results of the above research explained that the sample C electrode had a fast redox process, leading to good cycle stability.[31] The possible reason is that the hydroxyl radical (—OH) group of PVA can bind with more than one site of PPy chains and form interchain linkages of several PPy chains to form conjugated network.[32,33] This leads to better accommodation of volume changes during redox process. Although some fluctuations in the capacitance were encountered, the perfect stability of the composites was demonstrated at a low current density.

Electrochemical impedance spectroscopy (EIS) has been widely used to study the redox (charging/discharging) processes of electrode materials and to evaluate their electronic and ionic conductivities.[34] The Nyquist plots of the Ag/PPy composite electrodes prepared under different conditions (Figure 8), as well as the fitting results using an equivalent circuit are shown in Figure 9. In this equivalent circuit, R_s and charge transfer resistance (R_{ct}) are the ohmic resistance (total resistance of the electrolyte, separator, and electrical contacts) and charge transfer resistance, respectively.[35,36] CPE is the constant phase angle element, involving double-layer capacitance, and W represents the Warburg impedance. CPE is defined as:

$$Z_{CPE} = \left[Q^0(j\omega)^n\right]^{-1} \quad (2)$$

where Q^0 is the frequency-independent constant related to the surface and electroactive species, ω is the angular frequency, n arises from the slope of log$Z$ versus log$f$ plot. The values of n range from 0 to 1; $n = 1$ indicates the ideal capacitor behavior of CPE element, $n = 0$ indicates the resistor, and $n = 0.5$ indicates the Warburg behavior.[37]

Furthermore, the EIS was also carried out to prove the capacitive performance at the open-circuit potential in the frequency range of 0.01–100 Hz with AC-voltage amplitude of 5 mV. The typical Nyquist plots of Ag/PPy composites electrode are shown in Figure 8. In high-frequency intercept of the real axis, an internal resistance (R_s) can be observed, which included the resistance of the electrolyte, the intrinsic resistance of the active material, and the contact resistance at the interface active material/current collector.[38] The difference in the real part of the impedance between low and high frequencies could be used to evaluate the value of electrochemical charge transfer resistance (R_{ct}).[39] From comparing the diameters of the semicircles

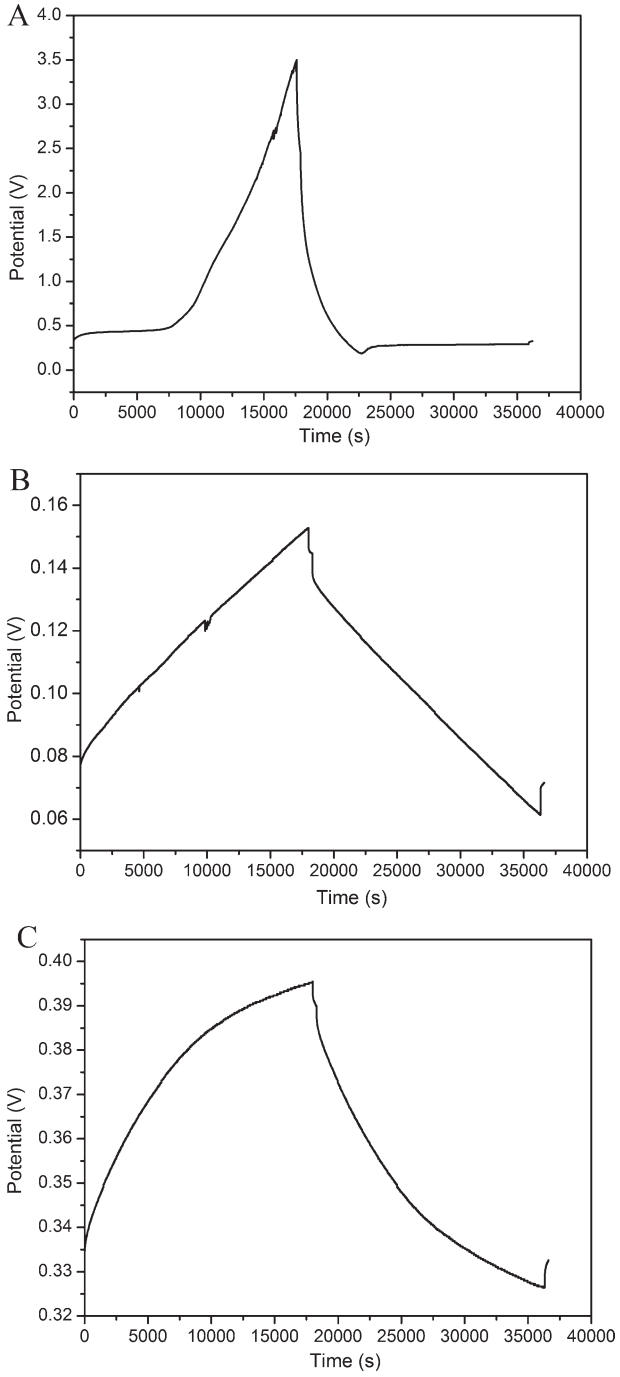

Figure 6. The charge–discharge curves of Ag/PPy electrodes at current densities of 2.45 mA/g (A, B, and C).

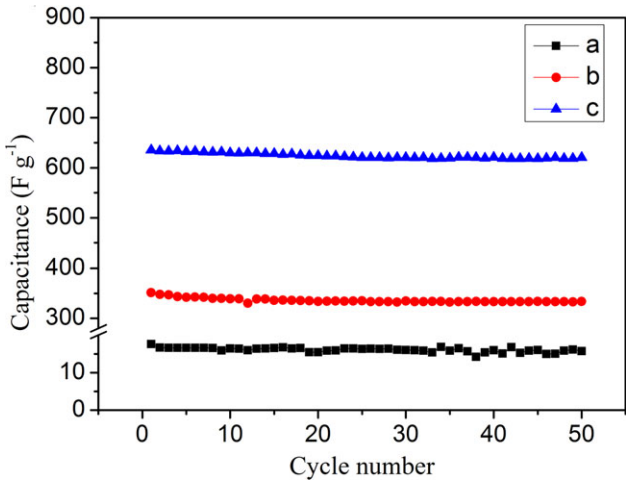

Figure 7. The specific capacitance of Ag/PPy electrodes at different galvanostatic charge–discharge cycle numbers. [Color figure can be viewed in the online issue, which is available at wileyonlinelibrary.com.]

(Figure 8), the charge transfer resistance (R_{ct}) of the sample C electrode is lower than those of the sample A and sample B electrode. The R_{ct} was calculated to be 2806, 516, and 318 Ω/cm for the samples A, B, and C, respectively.[40–42]

CONCLUSIONS

Ag/PPy nanocomposites were successfully synthesized by facile interface polymerization with $AgNO_3$ as the redox in the presence of different dispersants at room temperature. The electrochemical performance of the different Ag/PPy composites electrodes had been evaluated by galvanostatic charge–discharge and EIS. A series tests showed that the dispersant had great influence on the size, morphology, structure, and electrochemical characteristics of the obtained products. The specific capacitance reached 635.5 F/g of the Ag/PPy nanocomposites at a constant current of 2.45 mA g^{-1} and retained 97% of the initial value after 50 cycles when PVA was used as the dispersant.

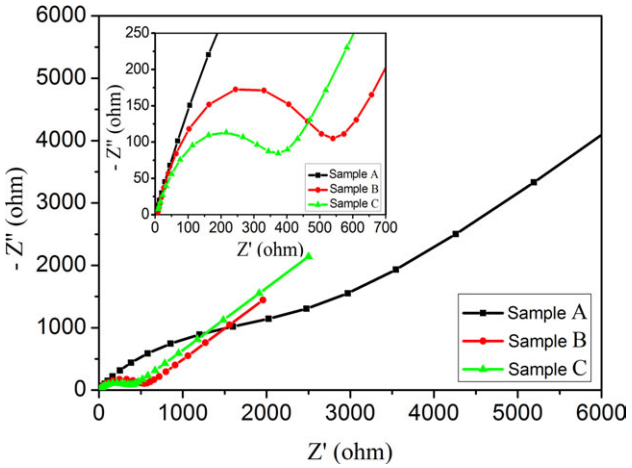

Figure 8. Nyquist impedance plots of the Ag/PPy electrodes. [Color figure can be viewed in the online issue, which is available at wileyonlinelibrary.com.]

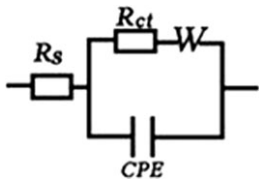

Figure 9. Equivalent circuit model.

These promising results, combined with the convenient and effective technique, make the composites an exceptional choice for electrode material of electrochemical supercapacitors.

ACKNOWLEDGMENTS

This study was supported by the College Scientific Plan Fund of Shandong Education Department (J10LD23) and the Doctoral Startup Foundation of Shandong Polytechnic University (12042826).

REFERENCES

1. Wang, S. B.; Shi, G. Q. *Chem. Phys.* **2007**, *02*, 255.
2. Chen, A. H.; Wang, H. Q.; Zhao, B. X.; Li, Y. *Synth. Met.* **2003**, *139*, 411.
3. Alqudami, A.; Annapoorni, S.; Se, P.; Rawat, R. S. *Synth. Met.* **2007**, *157*, 53.
4. Li, H. Y.; Wang, H. Q.; Chen, A. H.; Li, X. Y. *Mater. Chem.* **2005**, *15*, 2551.
5. Sadki, S.; Schottland, P.; Brodie, N.; Sabouraud, G. *Chem. Soc. Rev.* **2000**, *29*, 283.
6. Yan, F.; Xue, G.; Zhou, M. *J. Appl. Polym. Sci.* **2000**, *77*, 135.
7. Kim, D.; Choi, J.; Kim, J. Y.; Han, Y. K.; Shon, D. *Macromolecules* **2002**, *35*, 5314.
8. Han, D.; Chu, Y.; Yang, L.; Liu, Y.; Lv, Z. *Colloid. Surf. A* **2005**, *259*, 1793.
9. Gao, H.; Jiang,; Han, T. B.; Wang, Y.; Du, J.; Liu, Z.; Zhang, J. *Polymer* **2004**, *45*, 3017.
10. McCullough, R. D. *Adv. Mater.* **1998**, *10*, 93.
11. Kirkchmeyer, S.; Reuter, K. *J. Mater. Chem.* **2005**, *15*, 2077.
12. Skaff, H.; Sill, K.; Emrick, T. J. *Am. Chem. Soc.* **2004**, *126*, 11322.
13. Jang, J.; Oh, J. H.; Stucky, G. D. *Angew. Chem. Int. Ed.* **2002**, *41*, 4016.
14. Jing, S. Y.; Xing, S. X.; Yu, L. X.; Zhao, C. *Mater. Lett.* **2007**, *61*, 4528.
15. Selvan, S. T.; Spatz, J. P.; Klok, H. A.; Möller, M. *Adv. Mater.* **1998**, *10*, 132.
16. Lee, H.; Kim, H.; Cho, M. S.; Choi, J.; Lee, Y. *Electrochim. Acta* **2011**, *56*, 7460.
17. Lu, X. J.; Zhang, F.; Dou, H.; Yuan, C. Z.; Yang, S. D.; Hao, L.; Shen, L. F.; Zhang, L. J.; Zhang, X. G. *Electrochim. Acta* **2012**, *69*, 160.
18. Mi, H. Y.; Zhang, X. G.; Ye, X. G.; Yang, S. D. *J. Power Sources* **2008**, *176*, 403.

19. Sultana, I.; Rahman, M. M.; Wang, J. Z.; Wang C. Y.; Wallace, G. G.; Liu, H. K.; *Solid State Ionics* **2012**, *215*, 29.
20. Wang, J.; Xu, Y. L.; Chen, X.; Sun, X. F. *Compos. Sci. Technol.* **2007**, *67*, 2981.
21. Sahoo, S.; Nayak, G. C.; Das, C. K. *Macromol. Symp.* **2012**, *315*, 177.
22. Yin, Z.; Zheng, Q. D. *Adv. Energy Mater.* **2012**, *2*, 179.
23. Xu, Y. L.; Wang, J.; Sun, W.; Wang, S. H. *J. Power Sources* **2006**, *159*, 370.
24. Lu, X. J.; Dou, H.; Yuan, C. Z.; Yang, S. D.; Hao, L.; Zhang, F.; Shen, L. F.; Zhang, L. J.; Zhang, X. G. *J. Power Sources* **2012**, *197*, 319.
25. Hou, Y.; Chen, L. Y.; Zhang, L.; Kang, J. L.; Fujita, T.; Jiang, J. H.; Chen, M. W. *J. Power Sources* **2013**, *225*, 304.
26. Ding, K. Q.; Cheng, F. M. *Synth. Met.* **2009**, *159*, 2122.
27. Zhang, P. X.; Zhang, L.; Ren, X. Z.; Yuan, Q. H.; Liu, J. H.; Zhang, Q. L. *Synth. Met.* **2011**, *161*, 1092.
28. Oliveira, H. P.; Santos, M. V. B.; Santos, C. G.; Melo, C. P. *Mater. Charact.* **2003**, *50*, 223.
29. Sultana, I.; Rahman, M. M.; Li, S.; Wang, J. Z.; Wang, C. Y.; Wallace, G. G.; Liu, H. K. *Electrochim. Acta* **2012**, *60*, 201.
30. Madani, A.; Nessark, B.; Boukherroub, R.; Chehimi, M. M. *J. Electroanal. Chem.* **2011**, *650*, 176.
31. Han, F.; Li, D.; Li, W. C.; Lei, C.; Sun, Q.; Lu, A. H. *Adv. Funct. Mater.*, to appear, DOI: 10.1002/adf m.201202254.
32. Wei, L.; Sevilla, M.; Fuertes, A. B.; Mokaya, R.; Yushin, G. *Adv. Funct. Mater.* **2012**, *22*, 827.
33. Zhang, A. Q.; Xiao, Y. H.; Lu, L. Z.; Wang, L. Z.; Li, F. *J. Appl. Polym. Sci.*, to appear, DOI: 10.1002/APP.38153.
34. Nishihara, H.; Kyotani, T. *Adv. Mater.* **2012**, *24*, 4473.
35. Zhou, X. H.; Peng, C.; Chen, G. Z. *AlChE J.* **2012**, *58*, 974.
36. Shen, M. X.; Han, Y. Q.; Lin, X. C.; Ding, B.; Zhang, L. J.; Zhang, X. G. *J. Appl. Polym. Sci.*, to appear, DOI: 10.1002/APP.37958.
37. Chakraborty, G.; Gupta, K.; Rana, D.; Meikap, A. K. *Polym. Compos.*, to appear, DOI 10.1002/p c.22153.
38. Jayasree, R.; Chandrasekar, R.; Cindrella, L. *Polym. Compos.*, to appear, DOI 10.1002/pc.22285.
39. Ozkazanc, E.; Zor, S.; Ozkazan, H.; Gumus, S. *Polym. Eng. Sci.*, to appear, DOI: 10.1002/pen.233 63.
40. Kumar, M. S.; Bhat, D. K. *J. Appl. Polym. Sci.* **2009**, *114*, 2445.
41. Hosseini, M. G.; Bagheri, R.; Najjar, R. *J. Appl. Polym. Sci.* **2011**, *121*, 3159.
42. Jin, M.; Liu, Y. Y.; Li, Y. L.; Chang, Y. Z.; Fu, D. Y.; Zhao, H.; Han, G. Y. *J. Appl. Polym. Sci.* **2011**, *122*, 3415.